

Plasma-derived EV Phosphoproteomics through Chemical Affinity Purification

Anton Iliuk^{*1,2}, Xiaofeng Wu³, Li Li², Jie Sun⁴, Marco Hadisurya¹, Ronald S. Boris⁵ W. Andy Tao^{*1,2,3,4,6}

¹Department of Biochemistry, Purdue University, West Lafayette, IN 47907

²Tymora Analytical Operations, West Lafayette, IN 47906

³Department of Chemistry, Purdue University, West Lafayette, IN 47907

⁴College of Biological Science and Medical Engineering, Southeast University, Nanjing, China

⁵Department of Urology, Indiana University School of Medicine, Indianapolis, IN 46202

⁶Purdue Center for Cancer Research, Purdue University, West Lafayette, IN 47907

^{*}To whom correspondence should be addressed. Email: watao@purdue.edu; anton.iliuk@tymora-analytical.com

ABSTRACT

Invasive nature and pain caused to patients inhibit the routine use of tissue biopsy-based procedures for cancer diagnosis and surveillance. The analysis of extracellular vesicles (EVs) from biofluids have recently gained significant traction in the liquid biopsy field. EVs offer an essential “snapshot” of their precursor cells in real time and contain information-rich collection of nucleic acids, proteins, lipids, etc. The analysis of protein phosphorylation, as a direct marker of cellular signaling and disease progression, could be an important stepstone to successful liquid biopsy applications. Here, we introduce a rapid EV isolation method based on chemical affinity called EVtrap (Extracellular Vesicles Total Recovery and Purification) for EV phosphoproteomics analysis of human plasma. Incorporating EVtrap with high performance mass spectrometry (MS), we were able to identify over 16,000 unique peptides representing 2,238 unique EV proteins from just 5 μ L plasma sample, including most known EV markers, with substantially higher recovery levels compared to ultracentrifugation. Most importantly, more than 5,500 unique phosphopeptides representing almost 1,600 phosphoproteins in EVs were identified using only 1 mL of plasma. Finally, we carried out quantitative EV phosphoproteomics analysis of plasma samples from patients diagnosed with chronic kidney disease or kidney cancer, identifying dozens of phosphoproteins capable of distinguishing disease states from healthy controls. The study demonstrates the potential feasibility of our robust analytical pipeline for cancer signaling monitoring by tracking plasma EV phosphorylation.

KEY WORDS

Extracellular vesicles, exosomes, proteomics, phosphoproteomics, EVtrap, kidney cancer, renal cell carcinoma, LC-MS.

INTRODUCTION

Currently the most widespread method for clinical cancer profiling and disease diagnosis involves a tumor biopsy, an invasive and painful procedure, and one that certainly is impractical for early-stage detection. As certain cancer becomes a more chronic disease that requires active monitoring over longer periods of time, tissue biopsies on a continuous basis are no longer a realistic scenario. As a result, “liquid biopsies” – analysis of biofluids such as plasma, serum, urine – have gained much attention as a potentially useful source of diagnostic biomarkers.¹⁻⁴ Liquid biopsies offer numerous advantages for a clinical analysis, including non-invasive collection, suitable sample collection for longitudinal disease monitoring, better screenshot of tumor heterogeneity, higher stability and sample volumes, faster processing times, lower rejection rates and cost. However, there are technical challenges and shortcomings with the most common focus of liquid biopsy – circulating tumor cells (CTCs) and cell-free DNA (cfDNA) – including their heterogeneity, extreme rarity and high fragmentation levels.⁵⁻⁹

In addition, current analyses overwhelmingly focus on genetic information – usually gene mutations. While genetic testing is valuable, it could greatly benefit from an additional layer of biological information. The ability to detect the genome output – active proteins – can provide useful real-time information about the organism’s physiological functions and disease progression, particularly in cancer.¹⁰⁻¹³ Oncologists understand the value of protein testing and immunoassays and can easily interpret the results. Compared to gene panel testing, immunoassays, once developed, are relatively inexpensive and are easier to get adopted in clinical settings.

To help overcome some of the challenges associated with the current liquid biopsy methods a new field has generated a lot of interest over the past few years – profiling of cell-secreted extracellular vesicles (EVs, which include microvesicles and exosomes).^{14, 15} EVs provide an effective and ubiquitous method for intercellular communication, stimulation of immune system, removal of harmful materials and serve many more functions.¹⁶⁻¹⁸ As these are shed into every biological fluid and embody a good representation of their parent cell, analysis of the EV cargo has great promise for biomarker discovery and disease

diagnosis.^{19, 20} Previous studies also revealed that EV-based disease markers could be identified before the onset of symptoms or physiological detection of a tumor, making them promising candidates for early-stage disease detection.^{21, 22}

Despite the significant recent excitement and efforts, a standardized method for collecting and processing EVs has not yet been developed.²³ Differential centrifugation with ultracentrifugation (UC) as the final step is generally considered the “gold standard” for EV isolation (particularly for exosomes). However, this approach is highly time-consuming (typically 6-22 hours), requires dedicated equipment, and is low-throughput, thus not suitable in a clinical setting due to poor reproducibility.²⁴⁻²⁷ In addition, multiple studies have shown that the exosome recovery rate after ultracentrifugation is only 5-25%.²⁷⁻²⁹ Several other groups have published and commercialized new methods for EV isolation, which include polymer-induced precipitation,^{30, 31} antibody-based capture,^{32, 33} affinity filtration,³⁴ size-exclusion chromatography,^{29, 35} etc. However, each one has its own limitations, including low recovery rate (usually similar or slightly worse than ultracentrifugation) and high contamination levels,^{25-27, 29, 34, 36-40} While these can certainly be used as a faster alternative to UC, at 5-25% published yields, their efficiency of isolation still leaves much room for improvement. As result, there is a critical need for a fast, reproducible and inexpensive approach for EV isolation that would allow a much more complete capture and extraction of pure EVs for research and clinical purpose. This prerequisite is particularly essential for the analysis of active and tumor-specific proteins and phosphoproteins.

We have recently introduced a novel magnetic bead approach based on chemical affinity for urinary EV capture and purification.⁴¹ The technology, named EVtrap (Extracellular Vesicles total recovery and purification), enables complete capture of EVs onto beads modified with a combination of hydrophilic and aromatic lipophilic groups that have high affinity toward lipid-coated EVs. These modified amphiphilic beads are capable of capturing EVs with high purity, and we found that the method enables >95% recovery yield of all EVs present in the urine sample, a significant improvement compared to ultracentrifugation and commercial exosome isolation methods. We applied LC-MS analyses on proteins from EVs isolated by

1
2
3 EVtrap, and all known detectable exosome markers were significantly enriched after EVtrap compared to
4
5 UC. We also identified the largest number of phosphoproteins present in urinary EVs (>1,000
6
7 phosphoproteins in 10 mL of urine).
8
9

10 While the EVtrap approach showed a dramatic improvement in urinary EV analysis, blood is a
11
12 much more complex milieu with many more challenges in sample preparation and analysis. The scale of
13
14 free proteins and other molecules present in plasma or serum that affect EV analysis is orders of magnitude
15
16 higher than in urine. Nonetheless, blood contacts with most cells and organs, and is considered as the most
17
18 important biofluid for liquid biopsy. A majority of EVs from different types of cells are likely secreted into
19
20 the blood. Therefore, in order to enable blood-based liquid biopsy for disease diagnosis, in this study we
21
22 attempted to achieve EV isolation from plasma based on the EVtrap approach, with specific focus on EV
23
24 phosphoproteomics. We carried out a comparison between EVtrap, ultracentrifugation and other commonly
25
26 used exosome isolation methods. Using Western Blotting, silver staining and LC-MS analyses, we found
27
28 that EVtrap captured EV markers from plasma at significantly higher levels and improved EV capture purity
29
30 compared to UC and other standard EV isolation techniques.
31
32

33 We further utilized the EVtrap approach for EV phosphoproteome analysis from plasma. Protein
34
35 phosphorylation is a key control mechanism for cellular regulatory pathways, and one often targeted by
36
37 drug developers to create inhibitors that block signaling pathways involved in cancer and other diseases.
38
39 However, as far as liquid biopsy is concerned, phosphoproteins have been virtually ignored due to their
40
41 perceived instability and low abundance level in biofluids until our recent study.⁴² Phosphoproteins are
42
43 typically present at sub-stoichiometric levels, and thus the recovery rate during sample preparation steps
44
45 must be efficient in order to achieve their detection. To carry out EV plasma phosphoproteome analysis,
46
47 we utilized the EVtrap approach to capture EVs from 1 mL plasma sample and compared this method to
48
49 standard ultracentrifugation. We demonstrated efficient analysis of plasma phosphoproteome with the
50
51 EVtrap isolation method, and its feasible application for disease diagnosis.
52
53
54
55
56
57

Finally, we utilized our EVtrap-LCMS approach to examine EV proteome and phosphoproteome differences between healthy plasma controls and plasma samples from patients with chronic kidney disease and kidney cancer. These efforts resulted in discovery of several highly promising potential biomarkers for non-invasive detection of renal cell carcinoma from plasma, which we will further validate in upcoming studies.

EXPERIMENTAL SECTION

Experimental details on materials, ultracentrifugation, EV isolation by other methods, Western Blotting, silver staining, LC-MS analysis and data processing are included in the supporting information.

Sample collection

Plasma samples were collected under approval from Purdue University Human Research Protection Program and Indiana University Human Subjects Office Institutional Review Boards, and all patients were properly consented before samples were collected. All frozen samples were thawed and centrifuged 2,500 × g for 10 min to remove platelets, apoptotic bodies and other large particles and aggregates.

For EVtrap characterization experiments, we used plasma from healthy individuals. For the kidney cancer analysis part of the project, we used 1 mL each of plasma from: a) 5 healthy individuals (no known kidney-related disease); b) 5 patients with diagnosed chronic kidney disease (CKD), some of whom were also diagnosed with kidney stones; and c) 5 patients diagnosed with the most common form of kidney cancer - renal cell carcinoma (RCC).

Extracellular Vesicle Isolation by EVtrap

EVtrap beads were provided by Tymora Analytical as a suspension in water, and were used as described in more detail before.⁴¹ The plasma samples were diluted 20-fold in the diluent buffer and the EVtrap beads were added to the samples at 1:2 v/v ratio, and the samples incubated by end-over-end rotation for 30 min, according to manufacturer's instructions. After supernatant removal using a magnetic separator rack, the

beads were washed with PBS and the EVs eluted by a 10-min incubation with 200 mM triethylamine (TEA, Millipore-Sigma). The samples were fully dried in a vacuum centrifuge.

LC-MS Sample Preparation

The isolated and dried EV samples were lysed to extract proteins using the phase-transfer surfactant (PTS) aided procedure.⁴³ First, EVs were solubilized in the lysis solution containing 12 mM sodium deoxycholate, 12 mM sodium lauroyl sarcosinate, 10 mM TCEP, 40 mM CAA, and phosphatase inhibitor cocktail (Millipore-Sigma) in 50 mM Tris·HCl, pH 8.5 by incubating 10 min at 95°C. This step also denatured, reduced and alkylated the proteins. The samples were diluted fivefold with 50 mM triethylammonium bicarbonate and digested with Lys-C (Wako) at 1:100 (wt/wt) enzyme-to-protein ratio for 3 h at 37°C. Trypsin was added to a final 1:50 (wt/wt) enzyme-to-protein ratio for overnight digestion at 37°C. The samples were acidified with trifluoroacetic acid (TFA) to a final concentration of 1% TFA. Ethyl acetate solution was added at 1:1 ratio to the samples. The mixture was vortexed for 2 min and then centrifuged at 20,000 × g for 2 min to obtain aqueous and organic phases. The organic phase (top layer) was removed, and the aqueous phase was collected, dried down to <10% original volume in a vacuum centrifuge, and desalted using Top-Tip C18 tips (Glygen) according to manufacturer’s instructions. Each sample was split into 99% and 1% aliquots for phosphoproteomic and proteomic experiments respectively. The samples were dried completely in a vacuum centrifuge and stored at -80°C. For phosphoproteome analysis, the 99% portion of each sample was subjected to phosphopeptide enrichment using PolyMAC Phosphopeptide Enrichment kit (Tymora Analytical) according to manufacturer’s instructions, and the eluted phosphopeptides dried completely in a vacuum centrifuge. For phosphoproteomics analysis the whole enriched sample was used, while for proteomics only 50% of the sample was loaded onto LC-MS.

Data Availability

The mass spectrometry proteomics data have been deposited to the ProteomeXchange Consortium via the PRIDE⁴⁴ partner repository with the dataset identifier PXD017994.

RESULTS

Isolation of plasma EVs by EVtrap

Here, we adapted the EVtrap approach for purification of EVs from plasma samples. The collected and frozen plasma samples were thawed, and platelets and other large particles removed by centrifugation at $2,500 \times g$ for 10 minutes. The pre-cleared plasma samples were diluted 20-fold in PBS and incubated with EVtrap beads for 30 min.⁴¹ The captured EVs were eluted with 10-min incubation in 200mM triethylamine and the resulting EV samples dried in a vacuum centrifuge. Transmission Electron Microscopy (TEM) analysis showed the standard cup-shaped exosomes/microvesicles recovered (**Figure 1A,B**). Examination of the post-EVtrap eluted extracellular vesicles by Nanoparticle Tracking Analysis (NTA) and Tunable Resistive Pulse Sensing (TRPS) both demonstrated a similar range of the isolated EVs, with majority being in the 100-200 nm range (**Figure 1C,D**). The mode particle diameter was 137 nm and 134 nm, while d50 was 154 nm and 143 nm for NTA and TRPS respectively. While both methods showed pretty similar data, we found that TRPS produced more consistent and accurate results due to their nanopore-based single-particle analysis capabilities.

For the initial recovery yield comparison and method validation, we used $100K \times g$ ultracentrifugation “gold standard” as the control method (with and without PBS wash). An equivalent of 5 μ L plasma of the EV pellet from this ultracentrifugation (labeled as 100K UC) was loaded on the gel for Western Blot analysis. The supernatant after 100K UC was also further incubated with EVtrap beads to check if any residual exosome population was left in the supernatant after UC. Likewise, 5 μ L of direct plasma was used to capture EVs by EVtrap. After 30-min incubation the beads were washed and EVs were eluted and dried. Then the internal cargo was extracted by boiling in the LDS sample buffer (lithium dodecyl sulfate) and loaded on the gel. All samples were loaded on the same gel and detected by Western Blotting using a primary antibody against CD9 (a common exosome marker). The experiment was carried out 3 separate times for quantitation, with each isolation using a plasma from the same source (the complete blots for all three experiments are available in **Supplementary Figure S1**). A representative

1
2
3 Western Blot is shown in **Figure 2A**, and the quantitative values for each CD9 band signal are listed in the
4 bar graph in **Figure 2B**. For comparison, we also loaded 0.05 μ L of plasma (\sim 4 μ g protein; 1% of the
5 amount used by other methods), which, as expected, was too low to produce any detectable CD9 signal. As
6 the results show, ultracentrifugation step indeed captured only a portion of the exosomes (some were likely
7 lost during $10,000 \times g$ pre-treatment), with EVtrap being able to isolate and produce >7 -fold more CD9
8 signal. If EVtrap method is considered as capturing the majority of exosomes, then UC can be calculated
9 to capture \sim 14% of EVs on average - a recovery rate similar to other studies,^{27, 28} and equivalent to what we
10 found for urine EVs. Detection of EVs by EVtrap from the UC supernatant further confirmed the incomplete
11 isolation by UC, showing a large percentage of EVs remaining in the supernatant (**Figure 2**). We would
12 like to note that the high-yield capture by EVtrap was achieved after only a 45-min procedure, in
13 comparison to >5 hrs needed for the UC protocol.

24
25
26 Besides ultracentrifugation, we also sought to compare EVtrap method to other common EV
27 isolation approaches. We tested three common EV isolation kits – based on membrane affinity spin
28 method,³⁴ size-based filtration tube, and polymer-based exosome precipitation kit.³⁰ 100 μ L of plasma was
29 used in each case and 5 μ L equivalent was loaded on the same gel as the previous samples. As the results
30 in **Figure 2** demonstrate, the alternative methods produced somewhat similar or better exosome recovery
31 signal compared to 100K ultracentrifugation, matching the previously published results for these
32 methods.^{27, 29, 34, 37, 38} However, the low purity of these methods is a known disadvantage (as will also be
33 shown further in this study). Therefore, it is difficult to implement them for subsequent protein analysis due
34 to significant contamination from free plasma proteins. Nonetheless, EVtrap still produced the highest
35 exosome recovery yield compared to any other approach (**Figure 2A,B**). All CD9 band signals from the 3
36 replicate blots were quantified and mean signal intensities plotted on the bar graph in **Figure 2B** to show a
37 better comparison between the methods. The standard deviation error bars among EVtrap experiments are
38 higher than we expected, but this is likely because the 3 replicates were carried out on separate gels and the
39 Western Blotting analyses were also performed on separate membranes.

Our overall goal was to show how much of the EV amount can be obtained from the same volume of plasma. In many cases, the volume of clinical samples is very limited, and therefore the ability to enrich a high amount of EVs from a small volume would be very advantageous. This is the reason we compared the EV recovery in each method using the same starting volume. Nonetheless, it is common to assess the EV marker signal in relation to total protein amount. We carried out an additional experiment of CD9 Western Blot comparing the signal after EVtrap enrichment and 100K ultracentrifugation. Here, the recovered EVs were resuspended, lysed, and the concentration of each sample determined by Nanodrop. Then 5 μ g of each protein amount was loaded on a gel and analyzed with anti-CD9 antibody. As the data in the **Supplementary Figure S2** demonstrate, EVtrap again demonstrated a significant increase in CD9 signal when the loading sample amount was normalized by concentration.

Assessment of plasma EV purity

Besides EV capture yield analysis, another important feature is the purity of the isolated EVs. This is particularly important for plasma samples because the free proteins in plasma are present at 70-80 mg/mL, levels that can significantly impede biomarker analysis. To examine the amount of contamination by free plasma proteins present after each EV capture method, we used 5 μ L of plasma for each experimental treatment and detected the resulting EV sample with silver staining for total protein analysis. The samples were processed in the manner identical to those in the previous EV recovery experiments and loaded on the gel in the same sequence. As expected, 100K UC sample had lower level of contamination when compared to 0.05 μ L (1%) of direct plasma loaded, and much less after the PBS wash (**Figure 3A**). Three commercial kits tested (same as used in the first experiment) resulted in very high amount of contamination, and therefore low purity of EV isolation. When compared to 1% plasma sample loaded, all three commercial methods had >1% free protein contaminants remaining. As a result, these methods would be very difficult to use for downstream proteome and phosphoproteome analyses. Perhaps this is the primary reason why most researchers use them for DNA/RNA detection only. By comparison, EVtrap isolation showed the

cleanest sample compared to all three commercial products, and similar in contamination level compared to ultracentrifugation.

Examination of EVtrap reproducibility

In order to analyze clinical samples in high-throughput manner, a method must be able to demonstrate low experimental variability. Thus, we also tested EVtrap sample-to-sample reproducibility. The EVtrap reproducibility experiments were carried out using nine 10 μ L aliquots of plasma and the captured EV samples were then analyzed on the same blot using CD9 marker detection. The results shown in **Figure 3B** demonstrate outstanding sample-to-sample reproducibility with 3.2% coefficient of variation (CV). The expanded blot and the quantitative CD9 band values are shown in the **Supplementary Figure S3**.

LC-MS analysis of plasma EV proteome and phosphoproteome

For our preliminary phosphoproteome analyses, we used 1 mL of plasma for EVtrap capture and for ultracentrifugation as the control (100K UC; carried out after the $10,000 \times g$ centrifugation step). Our 100K ultracentrifugation method (total UC time \sim 5 hours, including 1 wash step) produced 321 unique phosphopeptides from 177 unique phosphoproteins (**Supplementary Table S1**). However, when EVtrap was used for 30-min capture, we saw a significant increase in phosphoproteome identification levels. We identified 5,570 unique phosphopeptides from 1,593 unique phosphoproteins using only 1 mL of plasma and a single 60-min LC-MS run (**Supplementary Table S2**). This confirms that most phosphoproteins were simply not detectable by MS after ultracentrifugation.

To complement our phosphoproteome data, we also carried out direct proteomics analysis from plasma EVs. For these samples, only 5 μ L equivalent of plasma was used. 100K UC procedure produced 3,282 peptides and 406 total proteins (**Supplementary Table S3**). EVtrap capture approach on the other hand allowed identification of 16,266 peptides from 2,238 unique proteins (**Supplementary Table S4**).

We further carried out label-free quantitation of EV proteins isolated by EVtrap and by UC. **Figure 4** shows the total signal increase of the identified proteins and phosphoproteins compared to UC (**Supplementary Table S5** and **S6**). In our experiment, we have identified 88 out of 100 common EV markers and proteins published in ExoCarta⁴⁵⁻⁴⁷ (marked EV protein data in **Supplementary Table S7**). Overall, the average signal increase in EV markers and total EV proteome level is 78-fold and 69-fold, respectively, for EVtrap compared to UC. This is noteworthy because many other studies have shown that different methods enrich different exosome populations with various success rates,^{38, 48} With EVtrap, it appears that the complete EV profile is recovered. Markedly, the overall increase in the phosphoproteome signal is ~85-fold. The significant increase in the phosphoproteome signal is due to most of the phosphopeptides being undetectable by LC-MS after ultracentrifugation, thus resulting in the relative abundance ratio of 100 (maximum set fold-change in Proteome Discoverer). This difference in intensities is substantial. While the internal RNA/DNA molecules and many proteins can still be detected even after low EV recovery, phosphoproteins are already present at very low concentrations. After poor sample preparation they would be essentially undetectable on a discovery instrument like mass spectrometer. These data confirmed our hypothesis that in order to achieve efficient identification and quantification of phosphoproteome in EVs, a method like EVtrap is necessary to enable simple and highly efficient EV isolation and recovery.

Finally, for purity comparison purpose, we also quantified the signal of serum albumin and other common high-abundant plasma proteins. The quantitative LC-MS data showed a similar intensity (ratio of 1.05) of serum albumin in the EV sample isolated by EVtrap compared to UC (**Figure 4**). When analyzing other high-abundant plasma proteins, the average increase in signal in the EVtrap sample was 1.48-fold (marked plasma protein data in **Supplementary Table S7**). While there is a small increase in contaminants level of about 1.48-fold after EVtrap capture, this increase is not significant compared to the 78-fold increase in EV markers and 69-fold increase in total EV protein amount. Therefore, it is apparent from these results that EVtrap indeed significantly improves protein and phosphoprotein detection from plasma

EVs without significantly increasing the level of contamination compared to the standard isolation methods like UC.

The data demonstrate that EVtrap can be applied to directly process plasma in only 30 minutes, which would be highly useful for routine clinical analysis. With 1 mL plasma being sufficient to identify over a thousand of phosphoproteins, and 5 μ L plasma enough to identify over two thousand unique proteins, the volume is also convenient for routine analysis.

EVtrap-based plasma EV phosphoproteome analysis of kidney cancer and CKD patient samples

Protein phosphorylation is a determining regulatory mechanism for pathological pathways directly linked to cancer and other diseases. With one previous study from our group unveiling the possibility of using plasma EV phosphoproteins as candidate biomarkers for breast cancer,⁴² we believe our novel benchmarked EVtrap technique allows a more efficient and robust way for phosphoprotein biomarker discovery using plasma EVs. Here, we focused on diseases related to kidney, including kidney cancer (specifically, renal cell carcinoma, RCC), which accounts for ~3% of human malignancies.⁴⁹ The currently most common methods of diagnosis include computerized tomography (CT) or computerized axial tomography (CAT) scan followed by invasive tumor biopsy, which are far from optimal.^{50, 51} In this study, we carried out preliminary efforts to detect potential biomarkers of kidney cancer using plasma EV samples to enable non-invasive diagnosis. The general workflow for the whole process of plasma EV proteome and phosphoproteome analysis is illustrated in **Figure 5**. In order to distinguish kidney cancer accurately from non-cancerous conditions, chronic kidney disease (CKD) patients plasma samples were included as an additional control in our study.⁵²

EVs were isolated from human plasma samples ($n = 5$ biological replicates/group \times 3 groups = 15), as described in **Figure 5** using our EVtrap approach. EV proteins were extracted and digested by trypsin with the aid of phase-transfer surfactants.⁴³ After detergent removal and desalting, 1.5% (~1 μ g) of each peptide sample was stored for direct proteome analysis. The remainder of each peptide sample was used for phosphopeptide enrichment with in-house developed PolyMAC dendrimer-based phosphopeptide

enrichment method⁵³ prior to LC-MS analysis. Both proteome and phosphoproteome fractions were analyzed on a Ultimate 3000 nanoLC coupled with Q Exactive HF-X mass spectrometer.⁵⁴ Additionally, indexed Retention Time Standard containing 11 artificial synthetic peptides was spiked into each sample and utilized as an internal standard to reduce run-to-run variations and assist with peptide quantitation.⁵⁵

This streamlined procedure resulted in identification of 146 significantly changing phosphoproteins and 28 significantly changing proteins in kidney cancer samples compared to control. Likewise, we identified 156 significantly changing phosphoproteins and 16 significantly changing proteins in CKD samples compared to control. Comparison between the RCC and CKD samples revealed 44 phosphoproteins and 10 proteins that are significantly different between these two groups. Overall quantitative proteomics and phosphoproteomics data are available in **Supplementary Tables S8 and S9**. Further, in-depth data analysis was employed to obtain statistical results and generate visualized hierarchical clustering groups (heatmaps) and volcano plots (**Figure 6**). The proteins and phosphoproteins included in the two heatmaps (6A and 6B) are listed in the **Supplementary Table S10**.

Hierarchical clustering analyses on quantitative proteomics and phosphoproteomics were performed on all individual biological replicates with the threshold of p-value at 0.05. Clusters of proteins or phosphoproteins with consistent significantly changing abundance levels among categories were highlighted and annotated on the right. For a more global visualization of the quantitation results, the volcano plots with basis of t test statistics featured the quantitative comparison analyses of the plasma EV proteomes (top) and phosphoproteomes (bottom) between every two sample categories out of three. Proteins and phosphoproteins with considerable up- and down-regulation in diseases were exposed through a t-test permutation-based FDR ($FDR = 0.05$, the horizontal dash line at $-\log(p\text{-value}) = 1.30$) and a difference on fold-change ($\text{fold-change} = 2$, the vertical dashed line at $\log_2(\text{ratio}) = \pm 1$), with all five biological replicates in each group being counted. Notably, a greater number of phosphoproteins were upregulated in disease states compared to control samples, a promising outcome for further clinical validation.

We focused on several significantly changing proteins and phosphoproteins and identified four

most promising biomarker representatives, with their relative abundances in three categories from DDA-mode quantitation sketched in linear box-and-whiskers plots (**Figure 7**). Indeed, prior studies substantiated the scientific rationale of these targets to be possible disease biomarkers. The anchoring function of cardiomyopathy-associated protein 5 (CMYA5) is corroborated to mediate the subcellular compartmentation of protein kinase A (PKA) by binding to PRKAR2A implicated in the STRING network analysis,^{56, 57} although no straightforward evidence yet exists underlining its cancer-correlated mechanism behind the abundance elevation (**Figure 7A**). Likewise, referring to KEGG database, the enhanced signal of Crk-like protein (CRKL) in phosphorylated form was supported by its critical role in PI3K-Akt signaling pathway in cancer formation (**Figure 7B**).^{58, 59} With regard to phosphoprotein LYRIC (MTDH) as a potential marker, it appears promising due to its interaction with the AKT1 and HRAS, both of which serve as key components in kidney carcinoma pathway. Moreover, the networks between MTDH and MMP9, MYC and ZBTB16 are also essential players in cancer progression (**Figure 7C**).⁵⁹ Beyond cancer-relevant roles, a previous finding of apolipoprotein A-IV (APOA4) as a concentration-increased protein in chronic renal disease underlines its feasibility as a kidney stone/inflammation-specific protein, which was mainly attributed to kidney metabolism (**Figure 7D**).⁶⁰ Additional linear box-and-whiskers plots for other potential candidates are shown in **Supplementary Figures S4-S6**.

DISCUSSION

Along with emerging research in EVs and exosomes, total EV and/or exosome capture and purification has been the focus of many recent studies that attempt to develop a simple and efficient EV isolation protocol. Here, we present a novel chemical affinity-based capture method for effective EV isolation from plasma. The EVtrap method enables the capture of complete EV profile based on the lipid bilayer structure of these vesicles and the unique combination of the hydrophilic and aromatic lipophilic groups on the synthesized beads. The binding of these combinatorial amphiphilic groups appears to be in part through the shift from hydrophilicity to amphiphilicity of these groups, electrostatic interactions and lipid affinity, and thus the EVs can be released with the increase in pH using TEA. The specificity of the

1
2
3 binding to the lipid bilayer membrane of EVs as opposed to free lipids and lipoproteins, as well as their
4 aggregates, is further enhanced by the additives in the diluent buffer.
5
6

7
8 We were able to isolate hundreds of phosphoproteins directly from plasma, and revealed its future
9 applications in the clinical settings. While our previous publication on plasma EV phosphoproteome
10 analysis produced strong data and demonstrated outstanding potential of this field,⁴² the EVtrap approach
11 would be more suitable for routine EV analysis and biomarker discovery from clinically-relevant samples.
12 The initial demonstration of this was implemented in this study of kidney cancer plasma EV
13 phosphoproteomics. We strongly believe that the future of disease detection will depend on robust and
14 reproducible analysis of low-abundant signaling proteins and phosphoproteins, especially for early cancer
15 diagnosis and monitoring. It will supplement the current assays and offer an additional layer of important
16 information not typically available from genetic tests.
17
18
19
20
21
22
23
24
25
26

27 Multiple studies have shown that there is a notable discordance between genomic information and
28 actual proteome/phosphoproteome profile, with phosphoprotein information being much more relevant for
29 cancer detection and molecular subtyping.^{10-12, 61, 62} A recent study published on breast cancer profiling
30 indicated the utility of phosphoproteomic data to help clarify the highly complex genomic features.⁶³ For
31 example, genomic data have not been successful in treatment decisions with MTOR and PI3K inhibitors
32 due to a myriad of mutations in multiple pathways, most not actionable.⁶⁴ Here, the researchers were able
33 to more confidently predict the drug response based on the phosphorylation of downstream signaling
34 targets. In another example, close to half of HER2-positive breast cancer patients do not respond well to
35 Herceptin.⁶⁵ Likewise, a significant number of HER2-negative women do respond to Herceptin.⁶⁶ In both
36 cases downstream phosphorylation analysis can predict these response differences. These examples
37 demonstrated the need to examine the more complete signaling pathways for better cancer subtyping in
38 addition to the presence of mutations or a receptor. Being able to do this in a less invasive manner using
39 plasma EV analysis would have an enormous public health benefit. Therefore, successful development of
40 methods like EVtrap will be a substantial step forward in this objective.
41
42
43
44
45
46
47
48
49
50
51
52
53
54
55
56
57
58
59
60

CONCLUSION

We have carried out a comprehensive assessment and comparison of the EVtrap method against several EV isolation methods for plasma proteome and phosphoproteome studies. The EVtrap method enables high recovery levels of exosomes with low contamination level and <5% CV. All detectable exosome markers were captured at higher levels than by the common ultracentrifugation approach. While most data in this study were generated using Western Blotting and LC-MS, the EVtrap-isolated vesicles can be used for different types of follow-up analyses. We expect that the captured EV cargo can also be processed for DNA/RNA examination. Because the proposed approach is magnetic beads based, it can be easily automated for a high-throughput screening or diagnostics assay in a hands-off manner. Researchers equipped with EVtrap will be able to uncover more low-abundant plasma biomarkers, such as those with post-translational modifications (PTMs). We hypothesize that low-abundant plasma EV proteins and phosphoproteins can one day be used for early-stage disease detection, longitudinal monitoring, and as companion diagnostics for targeted cancer treatments, particularly those involving kinase inhibitors.

ASSOCIATED CONTENT

Supporting Information

The Supporting Information is available free of charge on the ACS Publications website <http://pubs.acs.org>.

Supporting Experimental Section. (PDF)

Figure S1. Triplicate Western Blot results of comparison between Ultracentrifugation (UC), EVtrap and three commercial methods for exosome capture as in **Figure 2A**. (PDF)

Figure S2. Concentration-based comparison between ultracentrifugation (UC) and EVtrap. (PDF)

Figure S3. Expanded **Figure 3B**. (PDF)

Figure S4. Linear box-and-whiskers plots for select upregulated kidney cancer-specific phosphoproteins. (PDF)

Figure S5. Linear box-and-whiskers plots for select upregulated CKD-specific phosphoproteins. (PDF)

Figure S6. Linear box-and-whiskers plots for select upregulated CKD-specific proteins. (PDF)

Table S1. LC-MS phosphoproteome analysis data for 100K UC sample. (XLSX)

Table S2. LC-MS phosphoproteome analysis data for EVtrap sample. (XLSX)

Table S3. LC-MS proteome analysis data for 100K UC sample. (XLSX)

Table S4. LC-MS proteome analysis data for EVtrap sample. (XLSX)

Table S5. Quantitative proteomics results of LC-MS analyses for 100K UC and EVtrap samples. (XLSX)

Table S6. Quantitative phosphoproteomics results of LC-MS analyses for 100K UC and EVtrap samples. (XLSX)

Table S7. Marked EV proteins and abundant plasma proteins from quantitative proteomics results of LC-MS analyses for 100K UC and EVtrap samples (proteins only). (XLSX)

Table S8. Quantitative phosphoproteomics results of LC-MS analyses for normal control, chronic kidney disease and kidney cancer urine EV samples. (XLSX)

Table S9. Quantitative proteomics results of LC-MS analyses for normal control chronic kidney disease and kidney cancer urine EV samples. (XLSX)

Supplementary Table S10. Lists of proteins and phosphoproteins included in the two heatmaps in **Figures 6A and 6B.** (XLSX)

Supplementary Tables S1-13 Captions. (PDF)

AUTHOR INFORMATION

Corresponding Author

*watao@purdue.edu.

*anton.iliuk@tymora-analytical.com.

Author Contributions

The manuscript was written through contributions of all authors. All authors have given approval to the final version of the manuscript.

Notes

The authors declare competing financial interest. A.I. and W.A.T. are principals at Tymora Analytical Operations, which developed EVtrap beads and commercialized PolyMAC enrichment kit.

ACKNOWLEDGEMENT

We thank the IU Health ECRO Biorepository for help in obtaining specimens used in this study. All samples were collected under IRB approved protocol #1011004282 Development of a Biorepository for IU Health Enterprise Clinical Research Operations. We also would like to thank Thermo Fisher Scientific for providing our team with the Ultimate 3000 LC coupled with Q-Exactive HF-X high-resolution MS instrument, which enabled this research. Finally, we thank Dr. Anoop Pal and Izon Science for performing the TRPS analysis of the samples. This project has been funded in part by NIH grants R41CA210772, R44CA239845, and R43AG063589 (to A.I. and W.A.T.) and by the Walther Oncology Physical Sciences & Engineering Research Embedding Program (To W.A.T. and R.B.).

REFERENCES

1. Fernandez-Lazaro, D.; Garcia Hernandez, J. L.; Garcia, A. C.; Cordova Martinez, A.; Mielgo-Ayuso, J.; Cruz-Hernandez, J. J. Liquid Biopsy as Novel Tool in Precision Medicine: Origins, Properties, Identification and Clinical Perspective of Cancer's Biomarkers. *Diagnostics (Basel)* **2020**, *10*, (4).
2. Mattox, A. K.; Bettgowda, C.; Zhou, S.; Papadopoulos, N.; Kinzler, K. W.; Vogelstein, B. Applications of liquid biopsies for cancer. *Sci Transl Med* **2019**, *11*, (507).
3. Snow, A.; Chen, D.; Lang, J. E. The current status of the clinical utility of liquid biopsies in cancer. *Expert Rev Mol Diagn* **2019**, *19*, (11), 1031-1041.
4. Cervena, K.; Vodicka, P.; Vymetalkova, V. Diagnostic and prognostic impact of cell-free DNA in human cancers: Systematic review. *Mutat Res* **2019**, *781*, 100-129.
5. Kilgour, E.; Rothwell, D. G.; Brady, G.; Dive, C. Liquid Biopsy-Based Biomarkers of Treatment Response and Resistance. *Cancer cell* **2020**, *37*, (4), 485-495.
6. Nagrath, S.; Sequist, L. V.; Maheswaran, S.; Bell, D. W.; Irimia, D.; Ulkus, L.; Smith, M. R.; Kwak, E. L.; Digumarthy, S.; Muzikansky, A.; Ryan, P.; Balis, U. J.; Tompkins, R. G.; Haber, D. A.; Toner, M. Isolation of rare circulating tumour cells in cancer patients by microchip technology. *Nature* **2007**, *450*, (7173), 1235-1239.
7. Cohen, J. D.; Li, L.; Wang, Y.; Thoburn, C.; Afsari, B.; Danilova, L.; Douville, C.; Javed, A. A.; Wong, F.; Mattox, A.; Hruban, R. H.; Wolfgang, C. L.; Goggins, M. G.; Dal Molin, M.; Wang, T. L.; Roden, R.; Klein, A. P.; Ptak, J.; Dobbyn, L.; Schaefer, J.; Silliman, N.; Popoli, M.; Vogelstein, J. T.; Browne, J. D.; Schoen, R. E.; Brand, R. E.; Tie, J.; Gibbs, P.; Wong, H. L.; Mansfield, A. S.; Jen, J.; Hanash, S. M.; Falconi, M.; Allen, P. J.; Zhou, S.; Bettgowda, C.; Diaz, L. A., Jr.; Tomasetti, C.; Kinzler, K. W.; Vogelstein, B.; Lennon, A. M.; Papadopoulos, N. Detection and localization of surgically resectable cancers with a multi-analyte blood test. *Science* **2018**, *359*, (6378), 926-930.
8. Geurickx, E.; Hendrix, A. Targets, pitfalls and reference materials for liquid biopsy tests in cancer diagnostics. *Mol Aspects Med* **2020**, *72*, 100828.
9. Yan, W. T.; Cui, X.; Chen, Q.; Li, Y. F.; Cui, Y. H.; Wang, Y.; Jiang, J. Circulating tumor cell status monitors the treatment responses in breast cancer patients: a meta-analysis. *Sci Rep* **2017**, *7*, 43464.
10. Seviour, E. G.; Sehgal, V.; Lu, Y.; Luo, Z.; Moss, T.; Zhang, F.; Hill, S. M.; Liu, W.; Maiti, S. N.; Cooper, L.; Azencot, R.; Lopez-Berestein, G.; Rodriguez-Aguayo, C.; Roopaimoole, R.; Pecot, C. V.; Sood, A. K.; Mukherjee, S.; Gray, J. W.; Mills, G. B.; Ram, P. T. Functional proteomics identifies miRNAs to target a p27/Myc/phospho-Rb signature in breast and ovarian cancer. *Oncogene* **2016**, *35*, (6), 801.
11. Wulfkühle, J. D.; Berg, D.; Wolff, C.; Langer, R.; Tran, K.; Illi, J.; Espina, V.; Pierobon, M.; Deng, J.; DeMichele, A.; Walch, A.; Bronger, H.; Becker, I.; Waldhor, C.; Hofler, H.; Esserman, L.; Investigators, I. S. T.; Liotta, L. A.; Becker, K. F.; Petricoin, E. F., 3rd. Molecular analysis of HER2 signaling in human breast cancer by functional protein pathway activation mapping. *Clinical cancer research : an official journal of the American Association for Cancer Research* **2012**, *18*, (23), 6426-6435.
12. Li, J.; Zhao, W.; Akbani, R.; Liu, W.; Ju, Z.; Ling, S.; Vellano, C. P.; Roebuck, P.; Yu, Q.; Eterovic, A. K.; Byers, L. A.; Davies, M. A.; Deng, W.; Gopal, Y. N.; Chen, G.; von Euw, E. M.; Slamon, D.; Conklin, D.; Heymach, J. V.; Gazdar, A. F.; Minna, J. D.; Myers, J. N.; Lu, Y.; Mills, G. B.; Liang, H. Characterization of Human Cancer Cell Lines by Reverse-phase Protein Arrays. *Cancer cell* **2017**, *31*, (2), 225-239.
13. Pishvaian, M. J.; Bender, R. J.; Matrisian, L. M.; Rahib, L.; Hendifar, A.; Hoos, W. A.; Mikhail, S.; Chung, V.; Picozzi, V.; Heartwell, C.; Mason, K.; Varieur, K.; Aberra, M.; Madhavan, S.; Petricoin, E., 3rd; Brody, J. R. A pilot study evaluating concordance between blood-based and patient-matched tumor molecular testing within pancreatic cancer patients participating in the Know Your Tumor (KYT) initiative. *Oncotarget* **2016**.
14. Harel, M.; Oren-Giladi, P.; Kaidar-Person, O.; Shaked, Y.; Geiger, T. Proteomics of microparticles with SILAC Quantification (PROMIS-Quan): a novel proteomic method for plasma biomarker quantification. *Mol Cell Proteomics* **2015**, *14*, (4), 1127-1136.

15. Cocucci, E.; Meldolesi, J. Ectosomes and exosomes: shedding the confusion between extracellular vesicles. *Trends in cell biology* **2015**, *25*, (6), 364-372.
16. Milane, L.; Singh, A.; Mattheolabakis, G.; Suresh, M.; Amiji, M. M. Exosome mediated communication within the tumor microenvironment. *J Control Release* **2015**, *219*, 278-294.
17. Vader, P.; Breakefield, X. O.; Wood, M. J. Extracellular vesicles: emerging targets for cancer therapy. *Trends Mol Med* **2014**, *20*, (7), 385-393.
18. Lee, T. H.; D'Asti, E.; Magnus, N.; Al-Nedawi, K.; Meehan, B.; Rak, J. Microvesicles as mediators of intercellular communication in cancer--the emerging science of cellular 'debris'. *Semin Immunopathol* **2011**, *33*, (5), 455-467.
19. Lin, J.; Li, J.; Huang, B.; Liu, J.; Chen, X.; Chen, X. M.; Xu, Y. M.; Huang, L. F.; Wang, X. Z. Exosomes: novel biomarkers for clinical diagnosis. *TheScientificWorldJournal* **2015**, *2015*, 657086.
20. Xu, R.; Greening, D. W.; Zhu, H. J.; Takahashi, N.; Simpson, R. J. Extracellular vesicle isolation and characterization: toward clinical application. *The Journal of clinical investigation* **2016**, *126*, (4), 1152-1162.
21. Verma, M.; Lam, T. K.; Hebert, E.; Divi, R. L. Extracellular vesicles: potential applications in cancer diagnosis, prognosis, and epidemiology. *BMC Clin Pathol* **2015**, *15*, 6.
22. Yang, K. S.; Im, H.; Hong, S.; Pergolini, I.; Del Castillo, A. F.; Wang, R.; Clardy, S.; Huang, C. H.; Pille, C.; Ferrone, S.; Yang, R.; Castro, C. M.; Lee, H.; Del Castillo, C. F.; Weissleder, R. Multiparametric plasma EV profiling facilitates diagnosis of pancreatic malignancy. *Sci Transl Med* **2017**, *9*, (391), eaal3226.
23. Lotvall, J.; Hill, A. F.; Hochberg, F.; Buzas, E. I.; Di Vizio, D.; Gardiner, C.; Gho, Y. S.; Kurochkin, I. V.; Mathivanan, S.; Quesenberry, P.; Sahoo, S.; Tahara, H.; Wauben, M. H.; Witwer, K. W.; Thery, C. Minimal experimental requirements for definition of extracellular vesicles and their functions: a position statement from the International Society for Extracellular Vesicles. *Journal of extracellular vesicles* **2014**, *3*, 26913.
24. An, T.; Qin, S.; Xu, Y.; Tang, Y.; Huang, Y.; Situ, B.; Inal, J. M.; Zheng, L. Exosomes serve as tumour markers for personalized diagnostics owing to their important role in cancer metastasis. *Journal of extracellular vesicles* **2015**, *4*, 27522.
25. Witwer, K. W.; Buzas, E. I.; Bemis, L. T.; Bora, A.; Lasser, C.; Lotvall, J.; Nolte-'t Hoen, E. N.; Piper, M. G.; Sivaraman, S.; Skog, J.; Thery, C.; Wauben, M. H.; Hochberg, F. Standardization of sample collection, isolation and analysis methods in extracellular vesicle research. *Journal of extracellular vesicles* **2013**, *2*, 1-25.
26. Taylor, D. D.; Shah, S. Methods of isolating extracellular vesicles impact down-stream analyses of their cargoes. *Methods* **2015**, *87*, 3-10.
27. Nakai, W.; Yoshida, T.; Diez, D.; Miyatake, Y.; Nishibu, T.; Imawaka, N.; Naruse, K.; Sadamura, Y.; Hanayama, R. A novel affinity-based method for the isolation of highly purified extracellular vesicles. *Sci Rep* **2016**, *6*, 33935.
28. Lamparski, H. G.; Metha-Damani, A.; Yao, J. Y.; Patel, S.; Hsu, D. H.; Ruegg, C.; Le Pecq, J. B. Production and characterization of clinical grade exosomes derived from dendritic cells. *Journal of immunological methods* **2002**, *270*, (2), 211-226.
29. Stranska, R.; Gysbrechts, L.; Wouters, J.; Vermeersch, P.; Bloch, K.; Dierickx, D.; Andrei, G.; Snoeck, R. Comparison of membrane affinity-based method with size-exclusion chromatography for isolation of exosome-like vesicles from human plasma. *J Transl Med* **2018**, *16*, (1), 1.
30. Zeringer, E.; Li, M.; Barta, T.; Schageman, J.; Pedersen, K. W.; Neurauter, A.; Magdaleno, S.; Setterquist, R.; Vlassov, A. V. Methods for the extraction and RNA profiling of exosomes. *World J Methodol* **2013**, *3*, (1), 11-18.
31. Niu, Z.; Pang, R. T. K.; Liu, W.; Li, Q.; Cheng, R.; Yeung, W. S. B. Polymer-based precipitation preserves biological activities of extracellular vesicles from an endometrial cell line. *PLoS One* **2017**, *12*, (10), e0186534.

32. Mathivanan, S.; Lim, J. W.; Tauro, B. J.; Ji, H.; Moritz, R. L.; Simpson, R. J. Proteomics analysis of A33 immunoaffinity-purified exosomes released from the human colon tumor cell line LIM1215 reveals a tissue-specific protein signature. *Mol Cell Proteomics* **2010**, *9*, (2), 197-208.
33. Yoo, C. E.; Kim, G.; Kim, M.; Park, D.; Kang, H. J.; Lee, M.; Huh, N. A direct extraction method for microRNAs from exosomes captured by immunoaffinity beads. *Anal Biochem* **2012**, *431*, (2), 96-98.
34. Enderle, D.; Spiel, A.; Coticchia, C. M.; Berghoff, E.; Mueller, R.; Schlumpberger, M.; Sprenger-Haussels, M.; Shaffer, J. M.; Lader, E.; Skog, J.; Noerholm, M. Characterization of RNA from Exosomes and Other Extracellular Vesicles Isolated by a Novel Spin Column-Based Method. *PLoS One* **2015**, *10*, (8), e0136133.
35. Welton, J. L.; Webber, J. P.; Botos, L. A.; Jones, M.; Clayton, A. Ready-made chromatography columns for extracellular vesicle isolation from plasma. *Journal of extracellular vesicles* **2015**, *4*, 27269.
36. Tang, Y. T.; Huang, Y. Y.; Zheng, L.; Qin, S. H.; Xu, X. P.; An, T. X.; Xu, Y.; Wu, Y. S.; Hu, X. M.; Ping, B. H.; Wang, Q. Comparison of isolation methods of exosomes and exosomal RNA from cell culture medium and serum. *Int J Mol Med* **2017**, *40*, (3), 834-844.
37. Bijnsdorp, I. V.; Maxouri, O.; Kardar, A.; Schelfhorst, T.; Piersma, S. R.; Pham, T. V.; Vis, A.; van Moorselaar, R. J.; Jimenez, C. R. Feasibility of urinary extracellular vesicle proteome profiling using a robust and simple, clinically applicable isolation method. *Journal of extracellular vesicles* **2017**, *6*, (1), 1313091.
38. Royo, F.; Zuniga-Garcia, P.; Sanchez-Mosquera, P.; Egia, A.; Perez, A.; Loizaga, A.; Arceo, R.; Lacasa, I.; Rabade, A.; Arrieta, E.; Bilbao, R.; Unda, M.; Carracedo, A.; Falcon-Perez, J. M. Different EV enrichment methods suitable for clinical settings yield different subpopulations of urinary extracellular vesicles from human samples. *Journal of extracellular vesicles* **2016**, *5*, 29497.
39. Liang, L. G.; Sheng, Y. F.; Zhou, S.; Inci, F.; Li, L.; Demirci, U.; Wang, S. An Integrated Double-Filtration Microfluidic Device for Detection of Extracellular Vesicles from Urine for Bladder Cancer Diagnosis. *Methods Mol Biol* **2017**, *1660*, 355-364.
40. Van Deun, J.; Mestdagh, P.; Sormunen, R.; Cocquyt, V.; Vermaelen, K.; Vandesompele, J.; Bracke, M.; De Wever, O.; Hendrix, A. The impact of disparate isolation methods for extracellular vesicles on downstream RNA profiling. *Journal of extracellular vesicles* **2014**, *3*, 1-14.
41. Wu, X.; Li, L.; Iliuk, A.; Tao, W. A. Highly Efficient Phosphoproteome Capture and Analysis from Urinary Extracellular Vesicles. *J Proteome Res* **2018**, *17*, (9), 3308-3316.
42. Chen, I. H.; Xue, L.; Hsu, C. C.; Paez, J. S.; Pan, L.; Andaluz, H.; Wendt, M. K.; Iliuk, A. B.; Zhu, J. K.; Tao, W. A. Phosphoproteins in extracellular vesicles as candidate markers for breast cancer. *Proc Natl Acad Sci U S A* **2017**, *114*, (12), 3175-3180.
43. Masuda, T.; Tomita, M.; Ishihama, Y. Phase transfer surfactant-aided trypsin digestion for membrane proteome analysis. *J Proteome Res* **2008**, *7*, (2), 731-740.
44. Perez-Riverol, Y.; Csordas, A.; Bai, J.; Bernal-Llinares, M.; Hewapathirana, S.; Kundu, D. J.; Inuganti, A.; Griss, J.; Mayer, G.; Eisenacher, M.; Perez, E.; Uszkoreit, J.; Pfeuffer, J.; Sachsenberg, T.; Yilmaz, S.; Tiwary, S.; Cox, J.; Audain, E.; Walzer, M.; Jarnuczak, A. F.; Ternent, T.; Brazma, A.; Vizcaino, J. A. The PRIDE database and related tools and resources in 2019: improving support for quantification data. *Nucleic Acids Res* **2019**, *47*, (D1), D442-D450.
45. Keerthikumar, S.; Chisanga, D.; Ariyaratne, D.; Al Saffar, H.; Anand, S.; Zhao, K.; Samuel, M.; Pathan, M.; Jois, M.; Chilamkurti, N.; Gangoda, L.; Mathivanan, S. ExoCarta: A Web-Based Compendium of Exosomal Cargo. *J Mol Biol* **2016**, *428*, (4), 688-692.
46. Mathivanan, S.; Fahner, C. J.; Reid, G. E.; Simpson, R. J. ExoCarta 2012: database of exosomal proteins, RNA and lipids. *Nucleic Acids Res* **2012**, *40*, (Database issue), D1241-1244.
47. Simpson, R. J.; Kalra, H.; Mathivanan, S. ExoCarta as a resource for exosomal research. *Journal of extracellular vesicles* **2012**, *1*, 1-6.
48. Wang, T.; Anderson, K. W.; Turko, I. V. Assessment of Extracellular Vesicles Purity Using Proteomic Standards. *Anal Chem* **2017**, *89*, (20), 11070-11075.
49. Siegel, R. L.; Miller, K. D.; Jemal, A. Cancer statistics, 2019. *CA Cancer J Clin* **2019**, *69*, (1), 7-34.

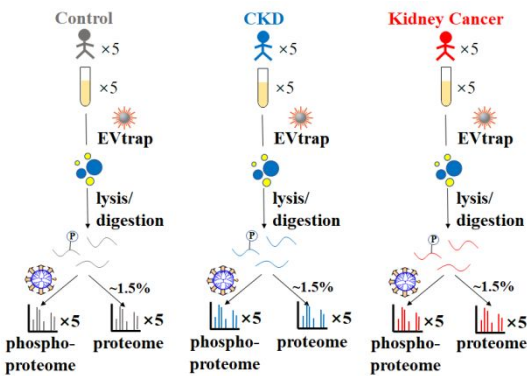
50. Ng, C. S.; Wood, C. G.; Silverman, P. M.; Tannir, N. M.; Tamboli, P.; Sandler, C. M. Renal cell carcinoma: diagnosis, staging, and surveillance. *AJR Am J Roentgenol* **2008**, *191*, (4), 1220-1232.
51. Diaz de Leon, A.; Pedrosa, I. Imaging and Screening of Kidney Cancer. *Radiol Clin North Am* **2017**, *55*, (6), 1235-1250.
52. Rule, A. D.; Bergstralh, E. J.; Melton, L. J., 3rd; Li, X.; Weaver, A. L.; Lieske, J. C. Kidney stones and the risk for chronic kidney disease. *Clin J Am Soc Nephrol* **2009**, *4*, (4), 804-811.
53. Iliuk, A. B.; Martin, V. A.; Alicie, B. M.; Geahlen, R. L.; Tao, W. A. In-depth analyses of kinase-dependent tyrosine phosphoproteomes based on metal ion-functionalized soluble nanopolymers. *Molecular & cellular proteomics* **2010**, *9*, (10), 2162-2172.
54. Kelstrup, C. D.; Bekker-Jensen, D. B.; Arrey, T. N.; Hoglebe, A.; Harder, A.; Olsen, J. V. Performance Evaluation of the Q Exactive HF-X for Shotgun Proteomics. *J Proteome Res* **2018**, *17*, (1), 727-738.
55. Collins, B. C.; Hunter, C. L.; Liu, Y.; Schilling, B.; Rosenberger, G.; Bader, S. L.; Chan, D. W.; Gibson, B. W.; Gingras, A. C.; Held, J. M.; Hirayama-Kurogi, M.; Hou, G.; Krisp, C.; Larsen, B.; Lin, L.; Liu, S.; Molloy, M. P.; Moritz, R. L.; Ohtsuki, S.; Schlapbach, R.; Selevsek, N.; Thomas, S. N.; Tzeng, S. C.; Zhang, H.; Aebersold, R. Multi-laboratory assessment of reproducibility, qualitative and quantitative performance of SWATH-mass spectrometry. *Nat Commun* **2017**, *8*, (1), 291.
56. Chursa, U.; Nunez-Duran, E.; Cansby, E.; Amrutkar, M.; Sutt, S.; Stahlman, M.; Olsson, B. M.; Boren, J.; Johansson, M. E.; Backhed, F.; Johansson, B. R.; Sihlbom, C.; Mahlapuu, M. Overexpression of protein kinase STK25 in mice exacerbates ectopic lipid accumulation, mitochondrial dysfunction and insulin resistance in skeletal muscle. *Diabetologia* **2017**, *60*, (3), 553-567.
57. Snel, B.; Lehmann, G.; Bork, P.; Huynen, M. A. STRING: a web-server to retrieve and display the repeatedly occurring neighbourhood of a gene. *Nucleic Acids Res* **2000**, *28*, (18), 3442-3444.
58. Tsuda, M.; Tanaka, S. Roles for crk in cancer metastasis and invasion. *Genes Cancer* **2012**, *3*, (5-6), 334-340.
59. Kanehisa, M.; Goto, S.; Furumichi, M.; Tanabe, M.; Hirakawa, M. KEGG for representation and analysis of molecular networks involving diseases and drugs. *Nucleic Acids Res* **2010**, *38*, (Database issue), D355-360.
60. Lingenhel, A.; Lhotta, K.; Neyer, U.; Heid, I. M.; Rantner, B.; Kronenberg, M. F.; Konig, P.; von Eckardstein, A.; Schober, M.; Dieplinger, H.; Kronenberg, F. Role of the kidney in the metabolism of apolipoprotein A-IV: influence of the type of proteinuria. *J Lipid Res* **2006**, *47*, (9), 2071-2079.
61. Chen, F.; Zhang, Y.; Parra, E.; Rodriguez, J.; Behrens, C.; Akbani, R.; Lu, Y.; Kurie, J. M.; Gibbons, D. L.; Mills, G. B.; Wistuba, II; Creighton, C. J. Multiplatform-based molecular subtypes of non-small-cell lung cancer. *Oncogene* **2017**, *36*, (10), 1384-1393.
62. Zagorac, I.; Fernandez-Gaitero, S.; Penning, R.; Post, H.; Bueno, M. J.; Mouron, S.; Manso, L.; Morente, M. M.; Alonso, S.; Serra, V.; Munoz, J.; Gomez-Lopez, G.; Lopez-Acosta, J. F.; Jimenez-Renard, V.; Gris-Oliver, A.; Al-Shahrour, F.; Pineiro-Yanez, E.; Montoya-Suarez, J. L.; Apala, J. V.; Moreno-Torres, A.; Colomer, R.; Dopazo, A.; Heck, A. J. R.; Altelaar, M.; Quintela-Fandino, M. In vivo phosphoproteomics reveals kinase activity profiles that predict treatment outcome in triple-negative breast cancer. *Nature communications* **2018**, *9*, (1), 3501.
63. Huang, K. L.; Li, S.; Mertins, P.; Cao, S.; Gunawardena, H. P.; Ruggles, K. V.; Mani, D. R.; Clauser, K. R.; Tanioka, M.; Usary, J.; Kavuri, S. M.; Xie, L.; Yoon, C.; Qiao, J. W.; Wrobel, J.; Wyczalkowski, M. A.; Erdmann-Gilmore, P.; Snider, J. E.; Hoog, J.; Singh, P.; Niu, B.; Guo, Z.; Sun, S. Q.; Sanati, S.; Kawaler, E.; Wang, X.; Scott, A.; Ye, K.; McLellan, M. D.; Wendl, M. C.; Malovannaya, A.; Held, J. M.; Gillette, M. A.; Fenyo, D.; Kinsinger, C. R.; Mesri, M.; Rodriguez, H.; Davies, S. R.; Perou, C. M.; Ma, C.; Reid Townsend, R.; Chen, X.; Carr, S. A.; Ellis, M. J.; Ding, L. Proteogenomic integration reveals therapeutic targets in breast cancer xenografts. *Nature communications* **2017**, *8*, 14864.
64. Mayer, I. A.; Abramson, V. G.; Isakoff, S. J.; Forero, A.; Balko, J. M.; Kuba, M. G.; Sanders, M. E.; Yap, J. T.; Van den Abbeele, A. D.; Li, Y.; Cantley, L. C.; Winer, E.; Arteaga, C. L. Stand up to cancer phase Ib study of pan-phosphoinositide-3-kinase inhibitor buparlisib with letrozole in estrogen receptor-

positive/human epidermal growth factor receptor 2-negative metastatic breast cancer. *Journal of clinical oncology : official journal of the American Society of Clinical Oncology* **2014**, 32, (12), 1202-1209.

65. Vogel, C. L.; Cobleigh, M. A.; Tripathy, D.; Gutheil, J. C.; Harris, L. N.; Fehrenbacher, L.; Slamon, D. J.; Murphy, M.; Novotny, W. F.; Burchmore, M.; Shak, S.; Stewart, S. J.; Press, M. Efficacy and safety of trastuzumab as a single agent in first-line treatment of HER2-overexpressing metastatic breast cancer. *Journal of Clinical Oncology* **2002**, 20, (3), 719-726.

66. Pogue-Geile, K. L.; Kim, C.; Jeong, J. H.; Tanaka, N.; Bandos, H.; Gavin, P. G.; Fumagalli, D.; Goldstein, L. C.; Sneige, N.; Burandt, E.; Taniyama, Y.; Bohn, O. L.; Lee, A.; Kim, S. I.; Reilly, M. L.; Remillard, M. Y.; Blackmon, N. L.; Kim, S. R.; Horne, Z. D.; Rastogi, P.; Fehrenbacher, L.; Romond, E. H.; Swain, S. M.; Mamounas, E. P.; Wickerham, D. L.; Geyer, C. E.; Costantino, J. P.; Wolmark, N.; Paik, S. Predicting Degree of Benefit From Adjuvant Trastuzumab in NSABP Trial B-31. *Jnci-J Natl Cancer I* **2013**, 105, (23), 1782-1788.

TOC only



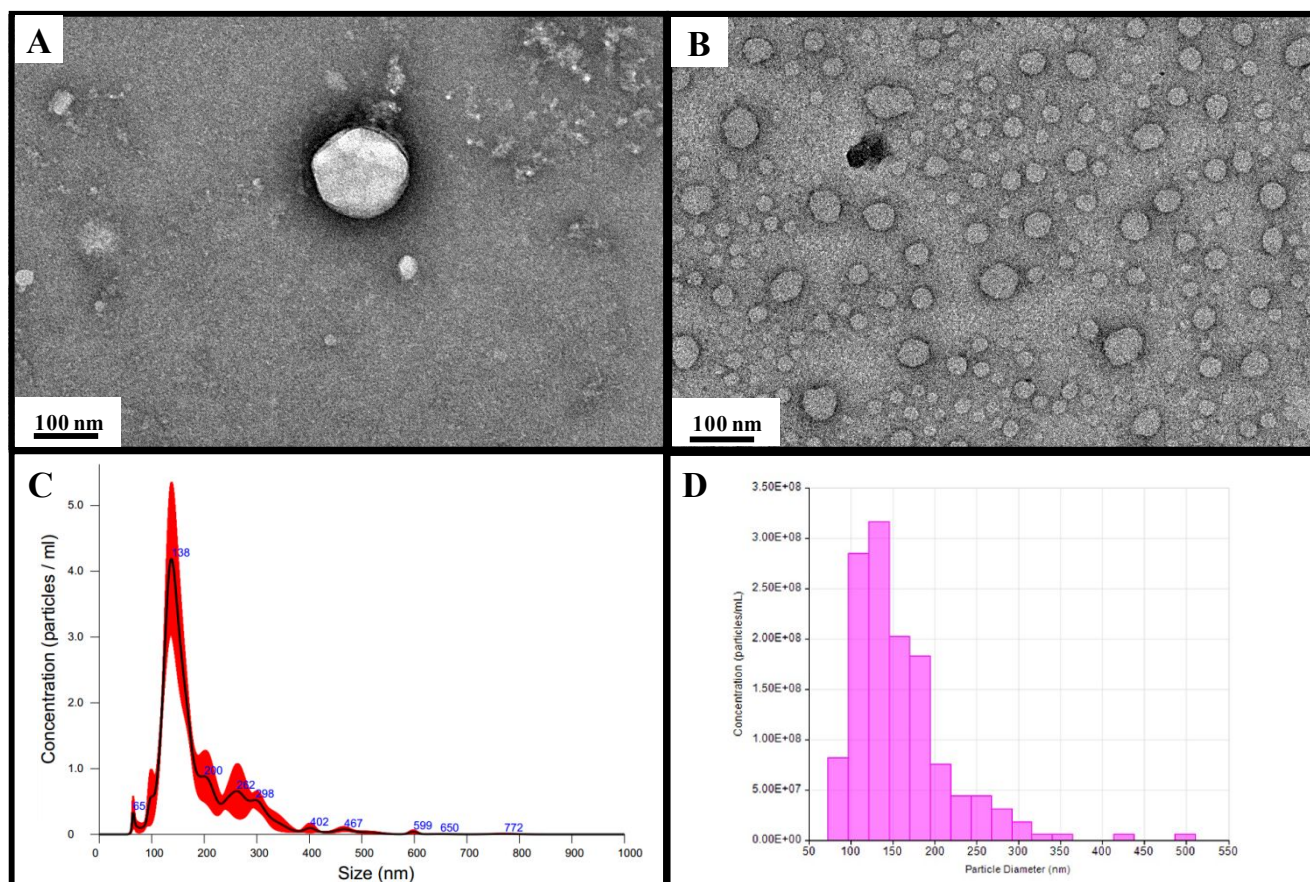


Figure 1. Transmission electron microscopy (TEM) images of A) single EV, and B) multiple EVs captured from the plasma by EVtrap. TEM imaging of EVs was carried out on a HITACHI H-8100 electron microscope (Hitachi, Tokyo, Japan) with an accelerating applied potential of 200 kV. C) Nanoparticle analysis using NTA after elution off EVtrap beads. D) Nanoparticle analysis using TRPS after elution off EVtrap beads.

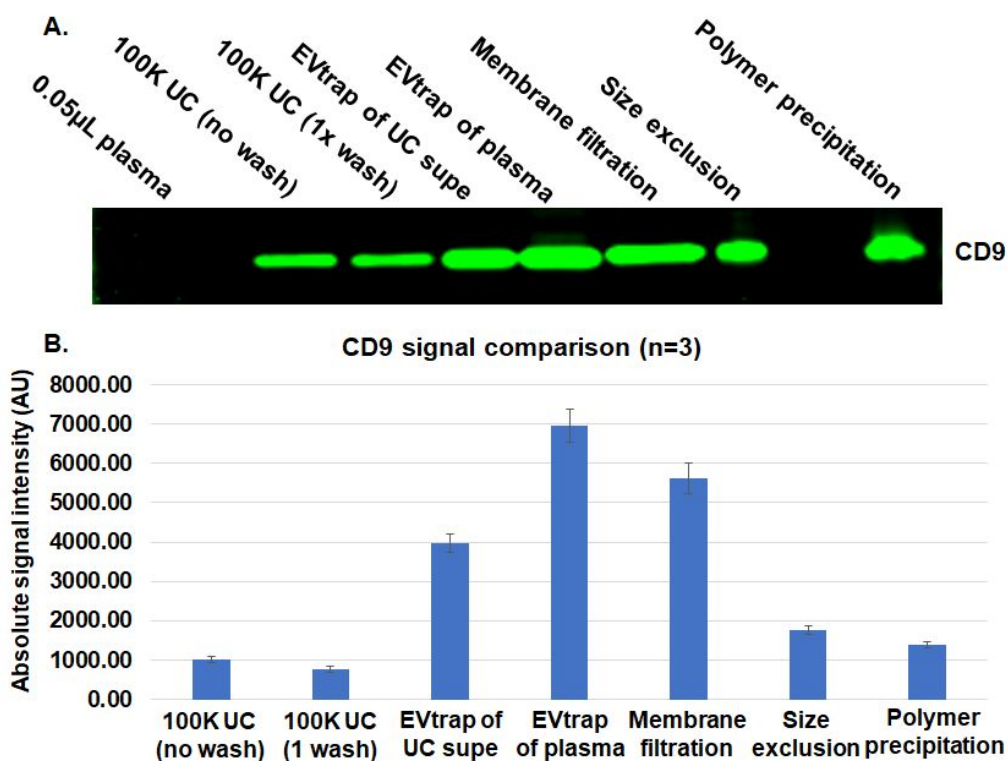


Figure 2. Comparison between ultracentrifugation (UC), EVtrap and 3 commercial methods for exosome capture. A) Detection of CD9 exosome marker using Western Blot. The lanes were loaded as follows: 0.05 μ L plasma loaded directly, EVs isolated from plasma by UC with no additional wash steps, EVs isolated from plasma by UC with 1 wash step, EVs captured by EVtrap from the UC supernatant sample (leftover after UC), EVs captured by EVtrap from plasma directly, EVs captured from plasma by membrane filtration method, EVs captured from plasma by size exclusion method, EVs captured from plasma by polymer precipitation method. All loaded EV samples were from 5 μ L plasma. B) Quantitation of WB data in (A) (n = 3).

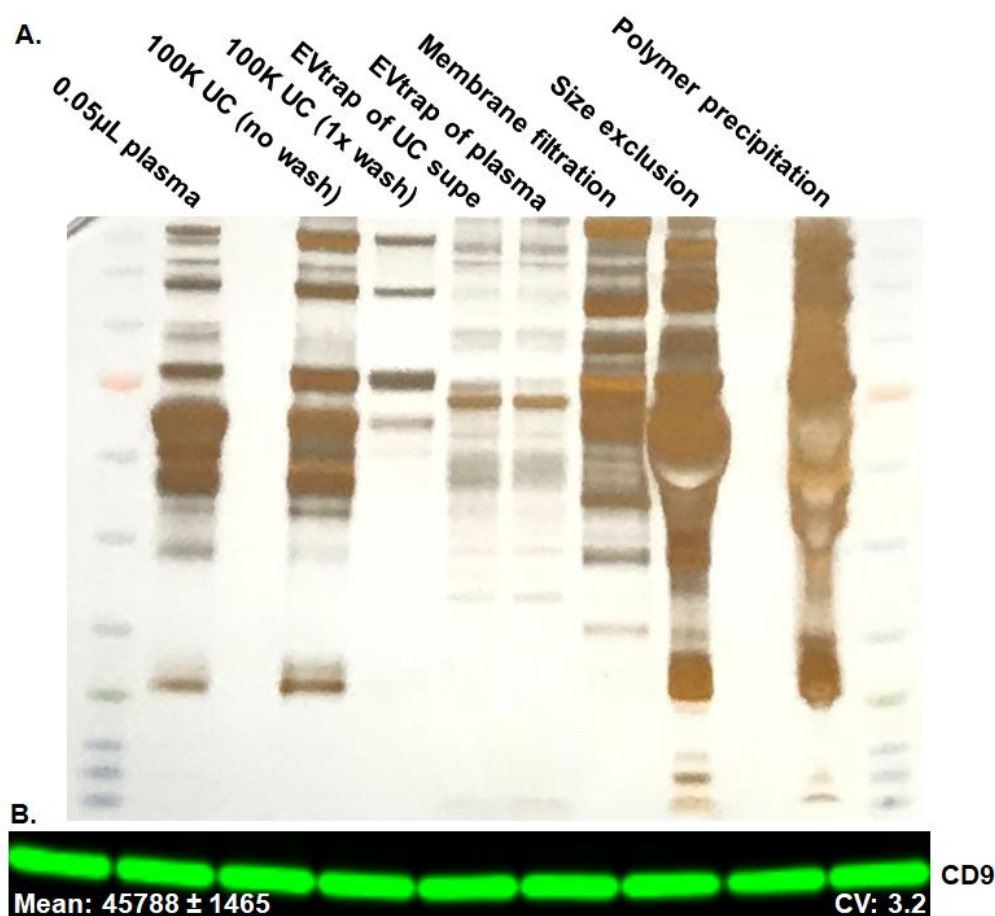


Figure 3. A) Silver stain total protein detection to assess plasma protein contamination. Comparison between ultracentrifugation (UC), EVtrap and 3 commercial methods for exosome capture. The lanes were loaded as follows: 0.05 μ L plasma loaded directly, EVs isolated from plasma by UC with no additional wash steps, EVs isolated from plasma by UC with 1 wash step, EVs captured by EVtrap from the UC supernatant sample (leftover after UC), EVs captured by EVtrap from plasma directly, EVs captured from plasma by membrane filtration method, EVs captured from plasma by size exclusion method, EVs captured from plasma by polymer precipitation method. All loaded EV samples were from 5 μ L plasma. B) Test of EVtrap procedure reproducibility carried using 9 separate plasma samples from the same source – detection of CD9 signal.

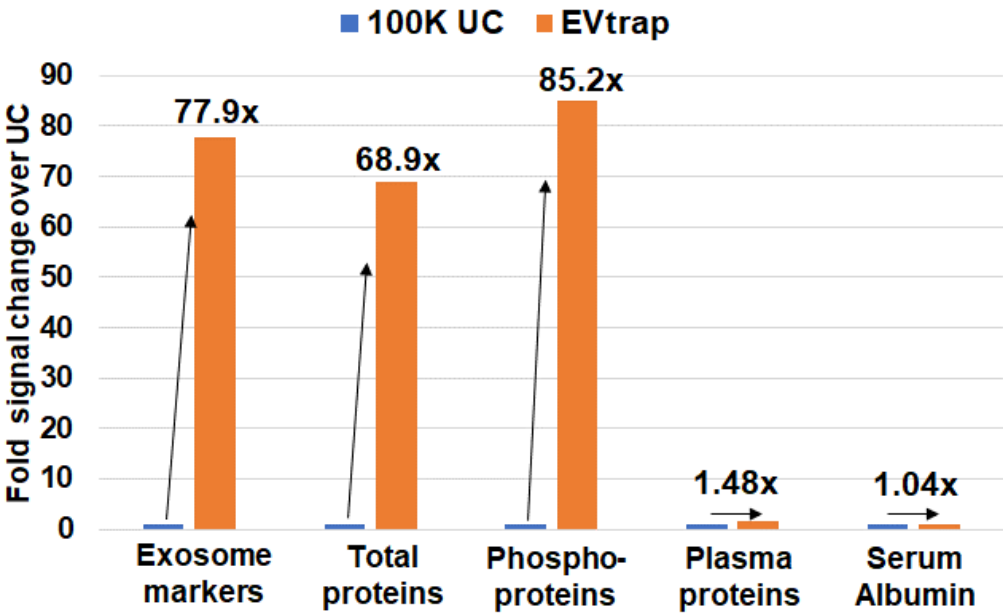


Figure 4. LC-MS proteome and phosphoproteome analyses of 100K UC and EVtrap samples. Fold change in overall signal between 100K UC and EVtrap experiments was quantified and plotted in a bar graph for: 88 identified common exosome markers, all proteins identified (excluding known contaminants), all phosphoproteins identified, serum albumin, and other high-abundant free plasma proteins (usually treated as contaminants).

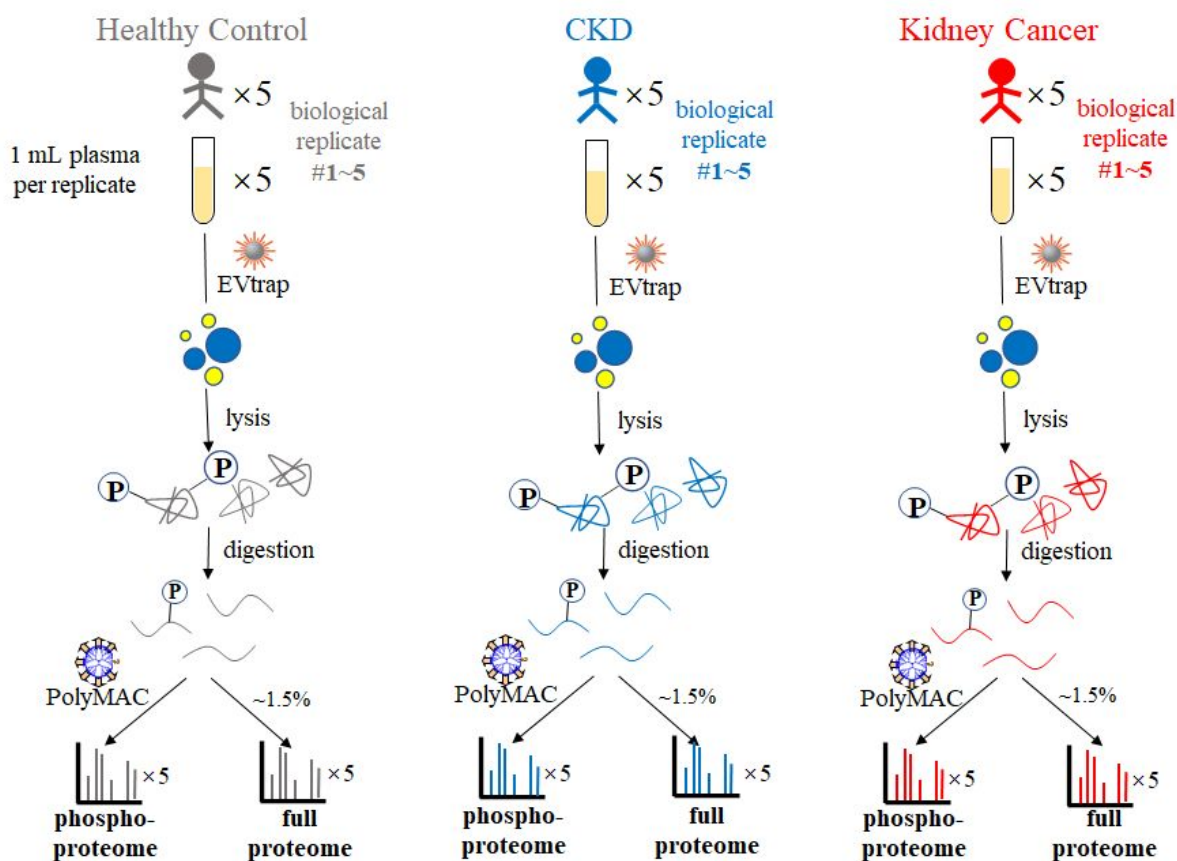


Figure 5. Workflow of EV proteomics and phosphoproteomics analyses of plasma samples from healthy controls, patients diagnosed with CKD and kidney cancer.

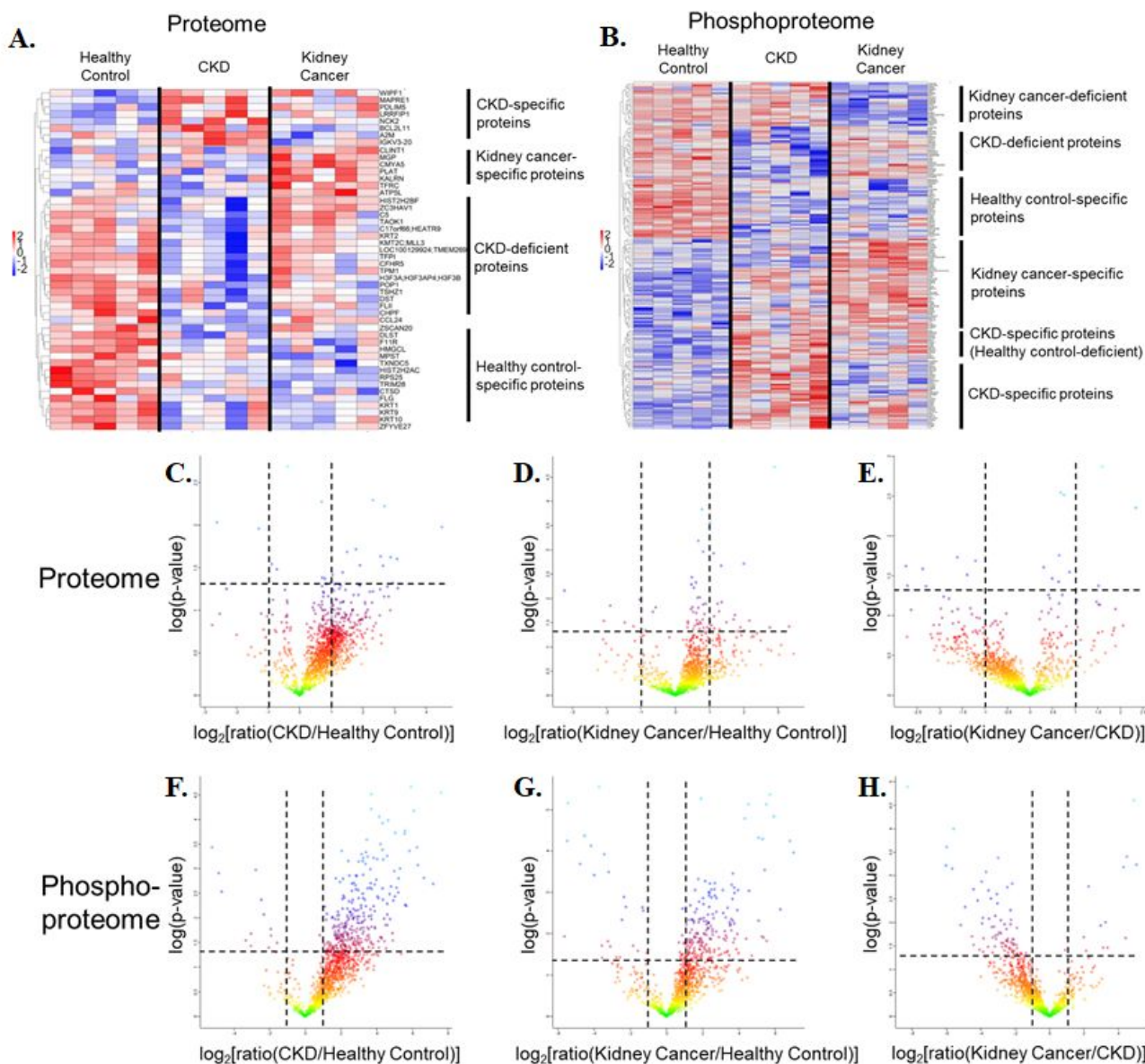


Figure 6. Hierarchical clustering analyses on quantitative proteomics (A) and phosphoproteomics (B) data. The gene names included in the two heatmaps (A) and (B) are listed in the Supplementary Table S10. C- H) The volcano plots representing the quantitative comparison of the plasma EV proteomes (top) and phosphoproteomes (bottom). Top: C) CKD vs. healthy control in full proteome; D) kidney cancer vs. healthy control in full proteome; E) kidney cancer vs. CKD in full proteome. Bottom: F) CKD vs. healthy control in phosphoproteome; G) kidney cancer vs. healthy control in phosphoproteome; H) kidney cancer vs. CKD in phosphoproteome.

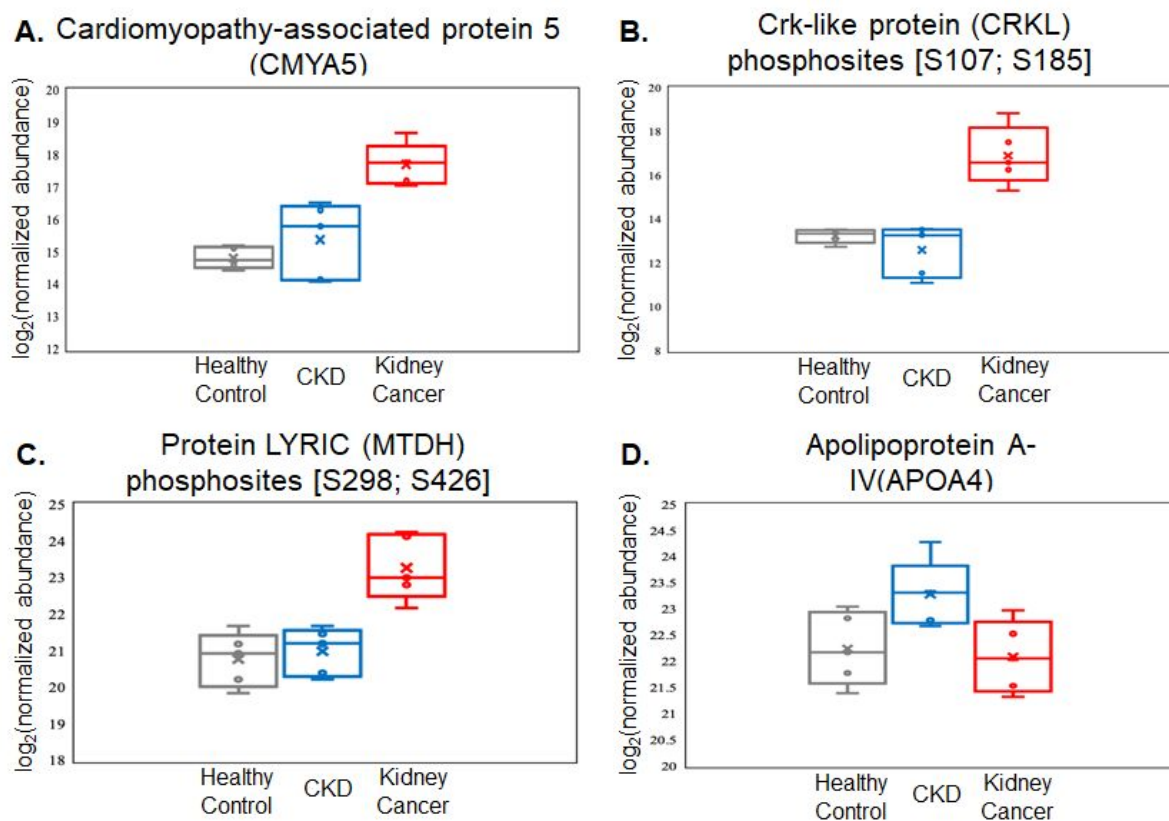


Figure 7. Relative abundance data of the selected four proteins and phosphoproteins as potential markers to differentiate the relevant categories. All four targets demonstrate significant upregulation ($P < 0.05$) in patients diagnosed with kidney cancer or CKD compared to the other two categories. A) kidney cancer-specific protein marker; B-C) kidney cancer-specific phosphoprotein markers; D) CKD-specific protein marker. All values are log₂ conversions of protein or phosphosite normalized abundance levels as determined by LC-MS.